Chapter 2

Phase behaviour of the CTAB–SHN–water system

2.1 Introduction

This chapter deals with the different liquid crystalline phases exhibited by cetyltrimethylammonium bromide (CTAB)– sodium-3-hydroxy-2-naphthoate (SHN)– water system. There have been some investigations on dilute solutions of this system mainly using electron and polarising microscopy, which revealed a cylinder to bilayer transition of the surfactant aggregates at [SHN]/[CTAB] $\sim$ 0.6. These earlier studies are discussed in section 2.2. We have characterized the mesophases of this system using x-ray diffraction and optical microscopy. At low SHN concentrations a hexagonal phase is observed. However at higher SHN concentrations, a rentrant lamellar (L_α^D) $\rightarrow$ centered rectangular (R) $\rightarrow$ lamellar (L_α) transition is found on decreasing the water content. These experimental observations are discussed in section 2.3. X-ray diffraction data indicate that the lamellar phase at low surfactant concentration (L_α^D) differs from that observed at high concentrations (L_α). The former structure (L_α^D) contains slits or pores in the plane of the bilayer. Some of the earlier experimental as well as theoretical studies on L_α^D to L_α transformations are described in section 2.4. In the L_α^D phase seen in other systems, the defects are found to disappear gradually on increasing the surfactant concentration. A similar behaviour is seen in the present system at high temperatures. However at low temperatures, a centred rectangular structure appears between the two lamellar phases. This is the first report of such a phase behaviour in surfac-

tant systems. This novel phase behaviour and other results of these studies are discussed in detail in section 2.5.

2.2 Earlier studies

Previous studies on the CTAB-SHN surfactant system were in the context of the formation of worm-like micelles [1]. At low surfactant concentrations (5 - 20 wt %) CTAB forms short rod-like micelles in aqueous solutions. The viscosity of these solutions remains low, nearly the same as that of water. Organic salts like sodium salicylate are known to induce the formation of 'worm-like' micelles in CTAB, which are long (~ 100 nm), flexible (persistence length ~ 10 nm) cylindrical micelles [2]. These micelles can become entangled to form a viscoelastic gel at low surfactant concentrations. NMR studies have shown that in CTAB-SHN micelles, the SHN molecule is oriented so as to keep its napthalene moiety in the hydrophobic region of the micelle. At α (=[SHN]/[CTAB]) ~ 0.67, a turbid, birefringent phase appears, followed by a thick birefringent precipitate at equimolar ratios of CTAB and SHN. The turbid phase was initially characterized as nematic using polarizing microscopy. However, subsequent studies on cetyltrimethylammonium 3-hydroxynaphthalene-2-carboxylate (CTAHNC) (obtained from equimolar ratios of CTAB and SHN) revealed the presence of vesicles and the birefringent phase was shown to be lamellar [3]. The vesicles could be transformed into worm-like micelles by shearing as well as by increasing the temperature [4]. The rich phase behaviour of these systems prompted Horbaschek et al. [5] to study the dilute CTAB-SHN system in detail. The sequence of phases seen in a 100 mM CTAB solution, on varying the SHN concentration, is summarized in table 2.1. Symmetry of the phase behaviour observed about the equimolar mixture is similar to that found in some mixed-surfactant systems [6].

On increasing the temperature of equimolar CTAB-SHN mixture, where a precipitate is observed at low temperatures, an isotropic to lamellar transition is found at 70^oC. Rheo-

Table 2.1: Phase behaviour of CTAB-SHN-water system at different SHN concentrations characterized through polarizing microscopy [5]. CTAB concentration in the dilute solution is 100 mM.

[SHN](mM)	Phase behaviour	no of Phases
50	isotropic viscoelastic gel	1
60	isotropic coacervate phase appears in the gel phase	2
> 60	lamellar phase appears in the coacervate phase	3
64	lamellar phase coexists with an isotropic phase	2
70	lamellar	1
> 90	appears turbid	1
100	a thick precipitate is formed	1
105	a turbid white suspension	1
119	turbidity decreases	1
120	isotropic and lamellar	2
122	an isotropic coacervate phase appears as the densest phase	3
140	lamellar phase disappears	2
150	isotropic phase	1

logical studies on the lamellar phase of the system show that the viscosity of this phase is much lower than that of the viscoelastic gel phase observed at lower SHN concentrations. No phase transitions are observed on shearing. Polarizing and electron microscopy on equimolar mixtures indicate multilamellar vesicles that stick together with an interlamellar distance less than 10 nm. Electron microscopy also reveals multilamellar vesicles, extended lamellar tubuli and stacks of bilayers in the lamellar phase.

Though dilute solutions of CTAB-SHN have been investigated in some detail, as discussed above, the phase behaviour of this system at higher surfactant concentrations has not been probed. Hence we have characterized the concentrated solutions using x-ray diffraction and polarizing microscopy.

2.3 Liquid crystalline phases of CTAB-SHN-water system

The phase behaviour was studied in detail at four different SHN concentrations corresponding to α = 0.25, 0.43, 0.67 and 1.0 . The total surfactant concentration was varied in the range

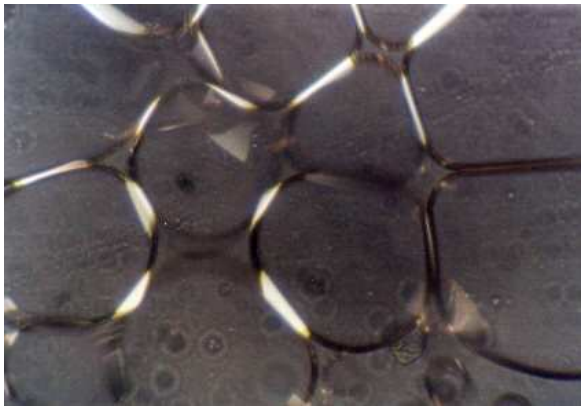

Figure 2.1: Flow birefringence of the isotropic phase of CTAB-SHN-water system ($\alpha = 0.25$) observed between crossed polarizers on shearing at 30 ^{o}C. The birefringence observed here (indicated by the bright regions) occurs due to the flow of the sample trapped between air bubbles.

10% to 80% by weight. At low SHN concentrations ($\alpha = 0.25$), an isotropic viscoelastic gel which is flow birefringent (fig 2.1) is observed at low surfactant concentrations. Microscopic observations show a texture characteristic of a hexagonal phase at ϕ_s [= wt of surfactant/(wt of water+surfactant)] ~ 0.4, at 30^oC (fig 2.5). X-ray diffraction shows two peaks in the small angle region with the magnitude of scattering vectors q in the ratio 1:$\sqrt{3}$ (fig 2.2a). These reflections correspond to the (1 0) and (1 1) planes of a 2D hexagonal lattice. These studies also indicate that the lattice parameter decreases as ϕ_s increases (table 2.3). On heating, no phase transitions occur in the system up to 90^oC. At very low water content, corresponding to $\phi_s \sim 0.7$, a crystalline phase appears at low temperatures, which on heating transforms to a hexagonal texture at 50^oC. The x-ray diffraction data consist of three peaks at 5.41 nm, 4.56 nm and at 2.28 nm (fig 2.2b). A long exposure in our experimental set up did not reveal any additional peaks. The presence of only two independent reflections makes it impossible to unambiguously determine the structure of this phase. Nevertheless, it is likely to be a rectangular phase. The phase diagram deduced from the data is given in fig 2.3. The d-spacings and the lattice parameters of the hexagonal phase are given in table 2.2.

On increasing the SHN concentration to $\alpha \sim 0.43$, an isotropic phase is observed at low surfactant concentrations (up to $\phi_s \sim 0.3$). Microscopic observations reveal that on increas-

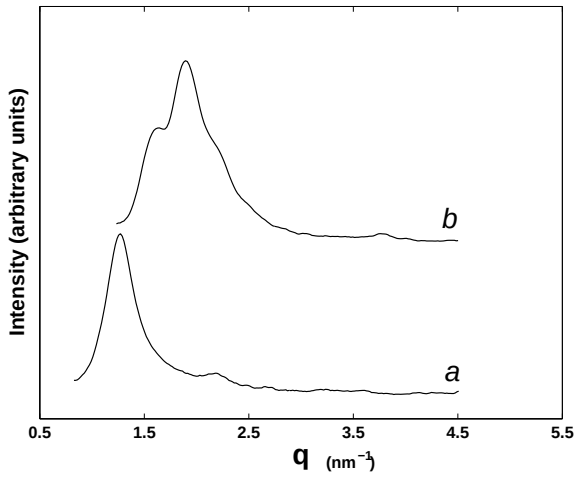

Figure 2.2: Diffraction data of CTAB-SHN-water system at α = 0.25, and ϕ_s = 0.5 (a); ϕ_s = 0.7 (b).

Table 2.2: The d-spacings, lattice parameters (a) and the mesophases in CTAB-SHN-water at α= 0.25 at 30^oC. ϕ_s is the total surfactant concentration (wt %).

ϕ_s	$d_1(nm)$	$d_2(nm)$	a (nm)	phase
40	6.13(s)		7.08	hexagonal
50	5.59(s)	3.22(w)	6.45	hexagonal
60	5.12(s)	2.96(w)	5.92	hexagonal

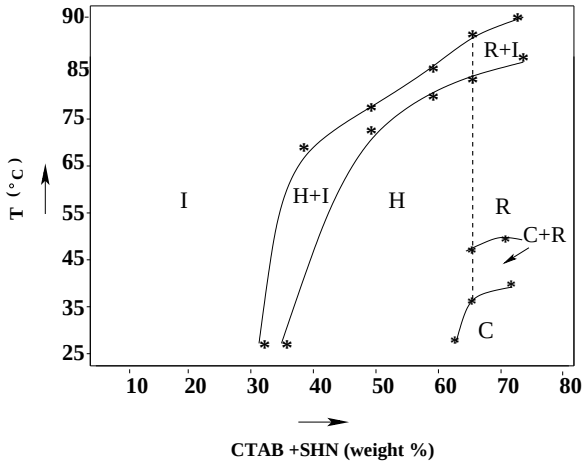

Figure 2.3: Phase diagram of CTAB-SHN-water system at α = 0.25. I, H, R and C denote the isotropic, hexagonal, rectangular and crystalline phases respectively.The boundary between the H and R regions has not been precisely determined.

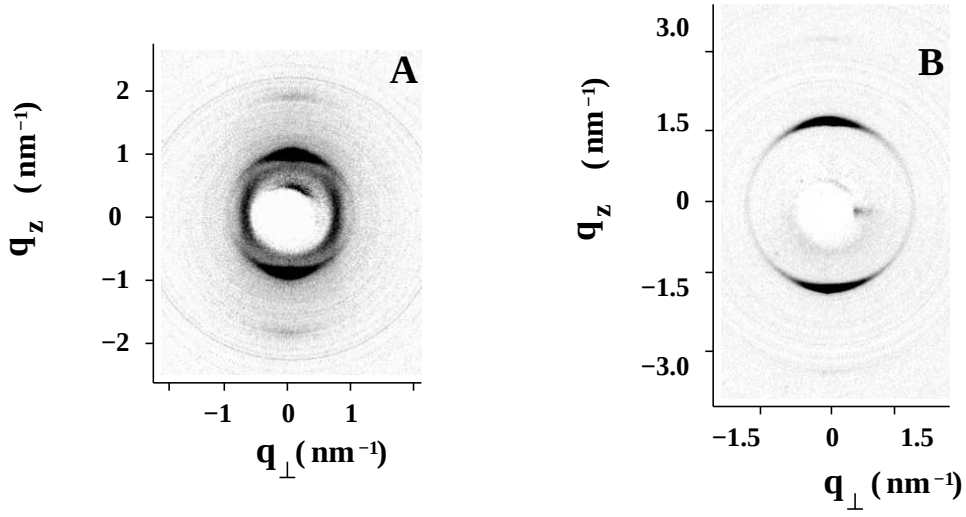

Figure 2.4: Typical diffraction patterns of a lamellar phase with defects (A) and a lamellar phase without defects (B). The diffraction pattern given here corresponds to α=1 and ϕ_s = 0.5 (A); 0.8 (B), though similar behaviour is seen at α = 0.43 and 0.67 .

ing the surfactant concentration, a lamellar texture (fig 2.6) coexists with the isotropic phase up to $\phi_s \sim 0.5$ at 30^{o}C. Thus a large coexistence region with the isotropic phase is observed here. On increasing the temperature, lamellar texture disappears leading to the formation of an isotropic phase. These solutions, unlike those at room temperature, were found to be highly viscous. The lamellar to isotropic transition temperature increases with the surfactant concentration. The lamellar texture is observed over a narrow range of surfactant concentration. Further increase of surfactant concentration to $\phi_s \sim 0.6$ leads to the appearance of two coexisting phases. The texture of one of them is lamellar. The other is similar to that seen in a hexagonal phase (fig 2.5). We refer to this henceforth in this chapter as the hexagonal texture though it may not be unique to the hexagonal phase. On heating they undergo a phase transition to a lamellar texture. With increase in ϕ_s, the transition temperature initially increases and later decreases. At $\phi_s \sim 0.7$, only a hexagonal texture is observed at 30 ^oC. On heating, transition to a lamellar texture occurs through a coexistence region. On cooling back to 30 ^{o}C, a typical texture appears which was not present before heating (fig 2.7). At high surfactant concentration, at around $\phi_s \sim 0.8$, a lamellar texture reappears at 30 ^{o}C (fig 2.8) .

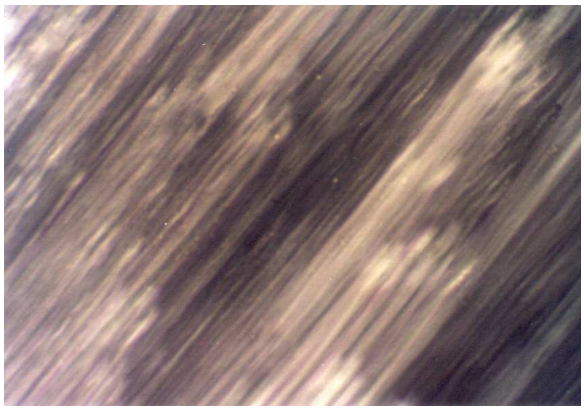

Figure 2.5: Typical texture of the hexagonal phase of CTAB-SHN-water system when observed between crossed polarizers at 30 ^oC.

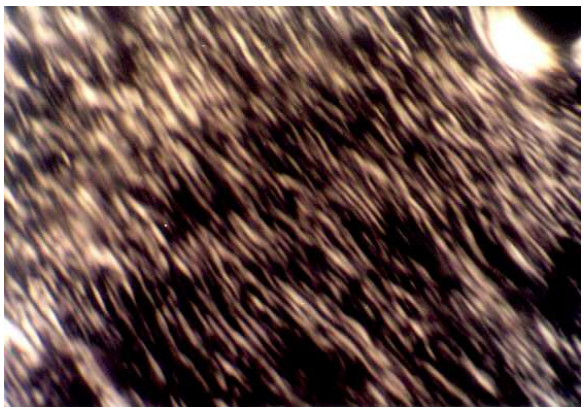

Figure 2.6: Typical texture of the lamellar phase with defects (L_α^D) when observed between crossed polarizers at 30 ^oC.

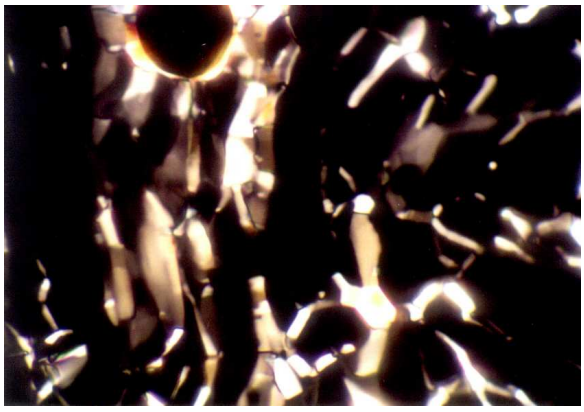

Figure 2.7: Typical texture of the ribbon phase (R) observed between crossed polarizers, on cooling from the L_α phase.

Figure 2.8: Typical texture of the lamellar phase without defects (L_α) when observed between crossed polarizers, at 30 ^oC.

The x-ray diffraction pattern of an oriented sample at ϕ_s = 0.5, shows two peaks with their q values in the ratio 1:2 (fig. 2.4A). These correspond to reflections from a lamellar structure. In addition, a diffused peak is observed at small angles, oriented perpendicular to the lamellar peaks. This peak corresponds to scattering from the plane of the bilayers. At $\phi_s \sim 0.6$, 6 peaks appear in the diffraction pattern. One of them, which is very weak, occurs at the same value as the first order lamellar peak at α = 0.5. The remaining 5 peaks can be indexed as the reflections from the (1 0), (0 1), (1 1), (1 $\overline{2}$) and (0 2) planes of a 2D oblique lattice. At $\phi_s \sim 0.7$, only two peaks occur. It is likely that these peaks also correspond to a 2D oblique lattice. At $\phi_s \sim 0.8$, one peak is observed in the small angle region. Since the microscopic studies indicate a lamellar texture, we conclude that this corresponds to a lamellar reflection. In the oriented sample of the lamellar phase, the diffuse peak oriented perpendicular to the lamellar peak is absent (fig. 2.4B). The phase diagram obtained from these studies is given in fig 2.9. The lattice parameters of the various structures are given in table 2.3.

Table 2.3: The lattice parameters and the mesophases in CTAB-SHN-water at α= 0.43 at 30^oC. vs, s, w and vw indicates the strength of the various reflections with vs being the strongest reflection and vw the weakest reflection. a b denote the lattice parameters.

ϕ_s (wt%)	d_1 (nm)	d_2 (nm)	d_3 (nm)	d_4 (nm)	d_5 (nm)	d_6 (nm)	a (nm)	b (nm)	γ	phase
40	5.72 (s)						5.72			L_α^D+I
45	5.35 (s)	2.68 (w)					5.35			L_α^D
50	5.24 (s)	2.59 (w)					5.24			L_α^D
60	7.03 (s)	5.24 (vw)	4.75 (vs)	3.29 (vw)	2.71 (vw)	2.39 (vw)	7.94	5.36	117.7^o	O+L_α^D
65	6.81 (s)	5.24 (vw)	4.7 (vs)	3.25 (vw)	2.64 (vw)	2.38 (vw)	7.61	5.36	116.5^o	O+L_α^D
70	6.08 (s)	4.51 (vs)								O
80	3.94 (s)							3.94		L_α

With further increase in SHN concentration to $\alpha \sim 0.67$, microscopic observations indicate an isotropic phase up to $\phi_s \sim 0.2$ at 30^oC. On increasing the surfactant concentration, we see the coexistence of a lamellar texture with the isotropic phase. The isotropic phase disappears at around $\phi_s \sim 0.4$. The lamellar texture persists up to $\phi_s \sim 0.55$ beyond which a hexagonal texture appears along with domains of lamellar texture. At $\phi_s = 0.6$ however only a hexagonal texture is observed. This remains so up to ϕ_s =0.7. Beyond this, a lamellar texture reappears. The phase behaviour observed on heating were found to be similar to that at $\alpha = 0.43$, described above (fig 2.10). At $\phi_s = 0.5$, the diffraction patterns of the oriented sample consists of three peaks in the small angle region. A diffused peak at around 7.8 nm is oriented perpendicular to two sharp peaks at 5.82 nm and 2.91 nm, which indicate a lamellar structure. But the peak positions do not shift on heating up to 60 ^{o}C. In our experimental set up the largest distances that can be measured is about 8 nm. Hence it is possible that the diffused peaks are present in the lamellar phase at lower surfactant concentrations, but have not been observed. At $\phi_s = 0.55$, the diffused peak is replaced by a sharp peak at 7.02 nm and a very strong peak at 5.29 nm. Three very weak reflections are also observed at 3.61 nm, 2.97 nm and 2.06 nm respectively. They could be indexed as the (2 0), (1 1), (3 1), (0

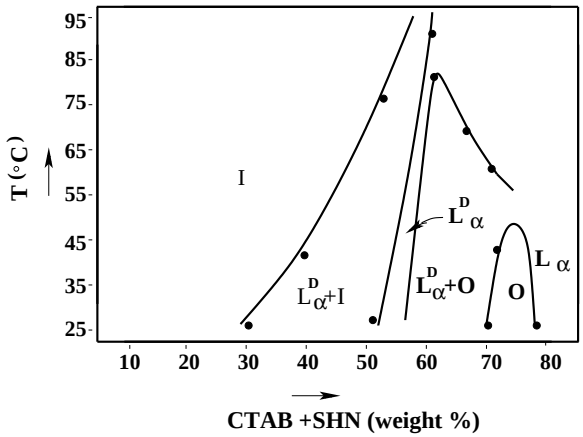

Figure 2.9: Phase diagram of CTAB-SHN-water system at $\alpha \sim 0.43$. L_α^D , O, $L_\alpha$and I denotes the lamellar phase with defects , a ribbon phase with a 2D oblique lattice, a lamellar phase without defects and the isotropic phase respectively.

Table 2.4: The d-spacings, lattice parameters and the mesophases in CTAB-SHN-water at α= 0.67 at 30^oC. *a* and *b* denote the lattice parameters.

ϕ_s	$d_1(nm)$	$d_2(nm)$	$d_3(nm)$	$d_4(nm)$	$d_5(nm)$	*a* (nm)	*b* (nm)	phase
42.5	6.89							L_α^D
45	6.35					6.35		L_α^D
47.5	5.97							L_α^D
50	7.8	5.82(s)	2.91(w)			5.82		L_α^D
52.5	7.66	5.49						L_α^D
55	7.02(s)	5.29(vs)	3.61(vw)	2.97(vw)	2.66(vw)	14.04	5.84	R
60	6.61(s)	4.88(vs)	3.31(vw)	2.73(vw)	2.44(vw)	13.0	5.42	R
70	6.08(s)	4.79(vs)	3.14(vw)	2.61(vw)	2.36(vw)	11.96	5.22	R
80	3.91(s)					3.91		L_α

2) and (2 2) reflections from a 2D centered rectangular lattice. However at $\phi_s \sim 0.8$, only one peak was observed at 3.91 nm (fig. 2.4B). Since the microscopic observations indicate a lamellar texture we can conclude that this peak arises from a lamellar structure. The lattice parameters of these phases at different surfactant concentrations are given in the table 2.4.

At low surfactant concentrations (ϕ_s = 0.1), a precipitate which phase separates at the top of the solution is seen in the CTAB-SHN mixture at $\alpha \sim 1.0$. Maltese crosses indicating the presence of multi-lamellar vesicles are observed under a polarizing microscope at 30^{o}C (fig 2.11). On heating, an isotropic phase is observed. When the surfactant concentration is

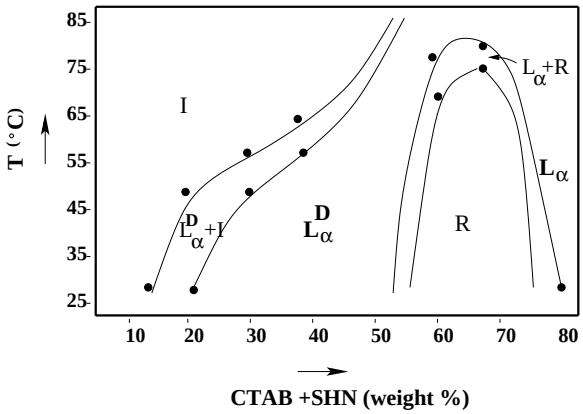

Figure 2.10: Phase diagram of CTAB-SHN-water system at $\alpha \sim 0.67$. L_α^D, R, L_α and I denotes the lamellar phase with defects, the centred rectangular phase, the lamellar phase without defects and the isotropic phase.

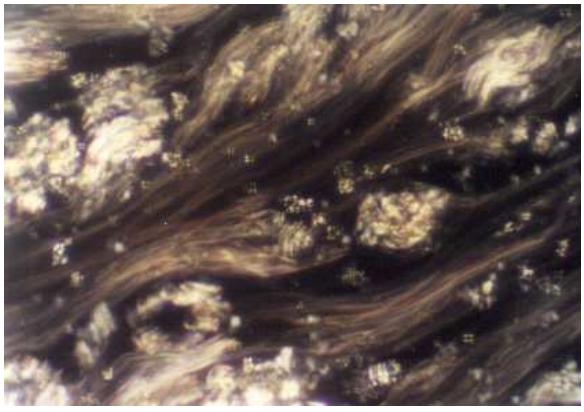

Figure 2.11: Typical texture of the multilamellar vesicles of the equimolar mixture of CTAB-SHN-water system ($\phi_s = 0.1$) when observed between crossed polarizers at 30^{o}C.

increased, the precipitate dissolves and the solution appears turbid. This behaviour persists up to $\phi_s \sim 0.3$. At $\phi_s = 0.3$, a lamellar texture is observed, which on heating transforms to an isotropic phase through a coexistence region. A similar phase behaviour is observed up to $\phi_s = 0.525$ beyond which a hexagonal texture appears. On heating, the hexagonal texture transforms into lamellar. At high surfactant concentrations a lamellar texture is observed ($\phi_s = 0.7$). Thus we find that though there is a shift in the phase boundaries as the SHN concentration is increased, the phase behaviour remains nearly the same in the range 0.43 $<\alpha < 1$.

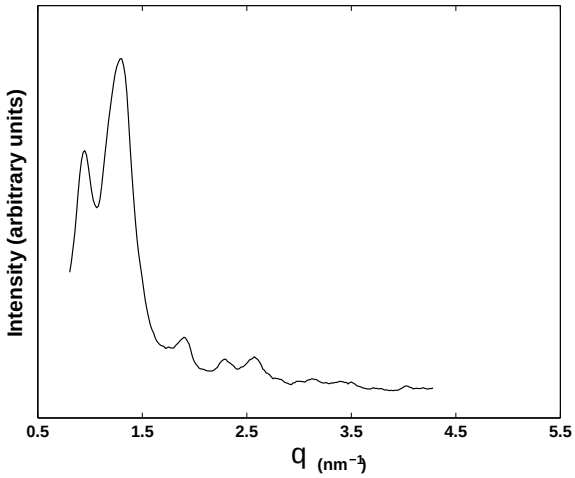

Figure 2.12: Diffraction data of CTAB-SHN-water system at $\alpha = 1$, $\phi_s = 0.6$.

X-ray diffraction studies at 30^{o}C of the CTAB-SHN mixture at $\phi_s = 0.1$ show two peaks at 4.81 nm and 2.4 nm indicating a lamellar phase (fig 2.4A). No diffraction peaks were observed up to 8 nm in the small angle region up to $\phi_s = 0.3$. At $\phi_s = 0.4$, two peaks observed in the small angle region consists of a strong reflection at 7.3 nm and a weak reflection at 3.65 nm, indicating a lamellar structure. On increasing the surfactant concentration, the diffraction pattern of the oriented sample shows two lamellar peaks and a diffuse peak oriented perpendicular to it. We also find that at similar surfactant concentrations, the diffuse peak occurs at larger angles for higher values of α. For example, at $\phi_s = 0.5$, the diffuse peak shifts from 7.8 nm at $\alpha = 0.67$ to 7.45 nm at $\alpha = 1.0$. At $\phi_s \sim 0.525$, five peaks are observed in the small angle region which can be indexed on a 2D centred rectangular lattice (fig 2.12). At $\phi_s \sim 0.7$, a strong reflection at 5.63 nm, a very strong reflection at 4.12 nm and a weak reflection at 2.06 nm are observed. Long exposure in our set up did not reveal additional peaks. Since microscopic studies indicate domains of lamellar and hexagonal textures, it is likely that the first peak corresponds to the (1 1) reflection of a centered rectangular phase. The second and third peaks would then correspond to a lamellar phase. The structures and their lattice parameters are tabulated below (table 2.5). The phase diagram is given in fig 2.13

Partial phase diagram of the tertiary CTAB-SHN-water system is shown in figure 2.14.

Table 2.5: The d-spacings, lattice parameters and the mesophases in CTAB-SHN-water at α= 1.0 at 30^oC. *a* and *b* denote the lattice parameters.

ϕ_s	$d_1(nm)$	$d_2(nm)$	$d_3(nm)$	$d_4(nm)$	$d_5(nm)$	*a* (nm)	*b* (nm)	phase
10	4.81(s)	2.4(w)				4.81		L_α^D+I
40	7.3(s)	3.65(w)				7.3		L_α^D
50	7.45	5.85(s)	2.93(w)			5.85		L_α^D
55	6.89(s)	5.51(vs)	3.68(vw)	2.75(vw)		13.78	6.0	R
60	6.55(s)	5.07(vs)	3.46(vw)	2.86(vw)	2.57(vw)	12.9	5.72	R
70	5.63(s)	4.12(vs)	2.06(w)					R+L_α

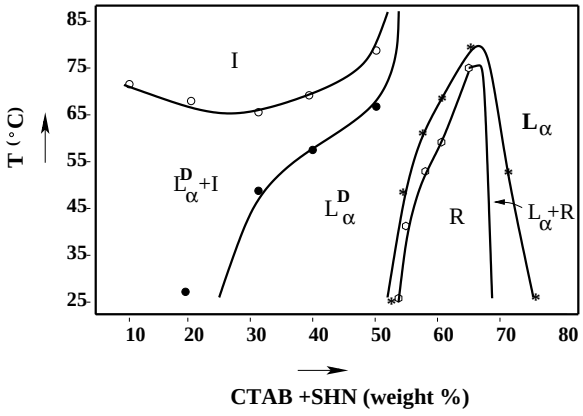

Figure 2.13: Phase diagram of CTAB-SHN-water system at equimolar ratios of CTAB and SHN. L_α^D, R, L_α denotes the lamellar phase with defects, centred rectangular phase and lamellar phase without defects respectively.

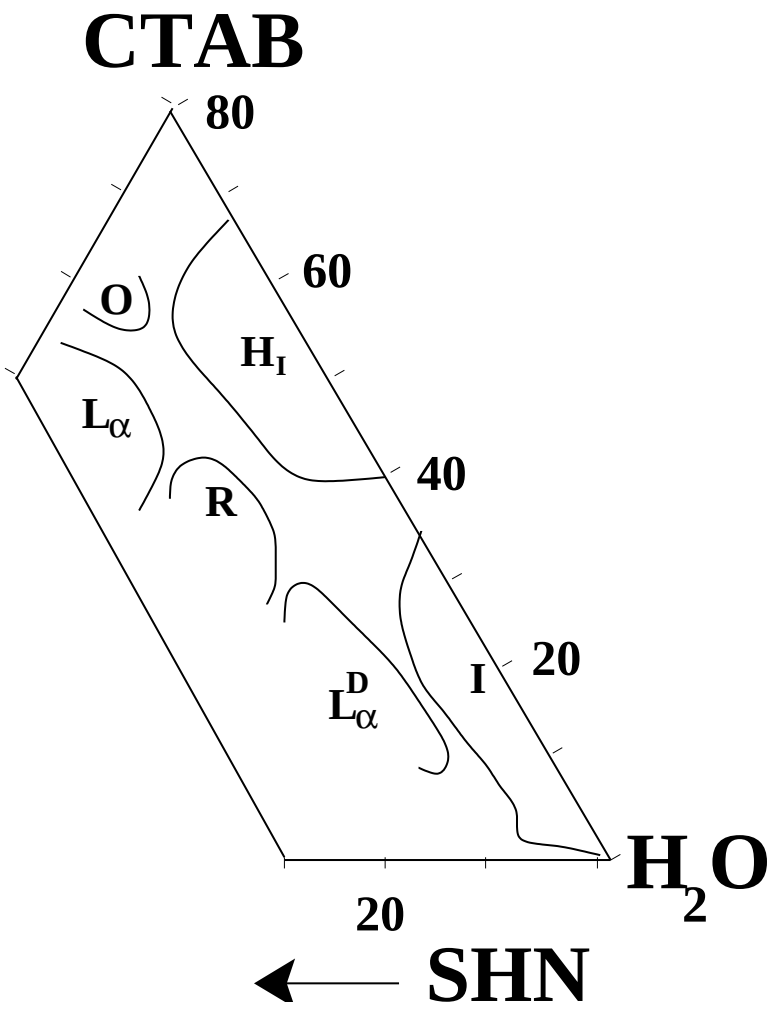

Figure 2.14: Partial phase diagram indicating the various liquid crystalline phases of CTAB-SHN-water system at 30 ^oC. L_α^D denotes the lamellar phase with defects, O denotes the 2D oblique phase, R the centred rectangular phase, I the isotropic phase, L_α the lamellar phase without defects and H, the hexagonal phase

Five single phase regions are found corresponding to the isotropic (I), hexagonal (H), rectangular (R), oblique (O), lamellar phases with and without defects (L_α^D, L_α). The presence of the 2D oblique phase in between H and L_α is similar to the phase behaviour seen in some surfactant systems [7]. However, as discussed below the formation of a 2D centred rectangular phase in between two lamellar phases has not been seen earlier.

2.4 Curvature defects in lamellar phases

Bilayers with pores or slits have been observed in some surfactant systems like cesium pentadecafluorooctanoate (CsPFO) -water [8]. CsPFO forms disk-like micelles in dilute solutions, which become orientationally ordered to give a nematic phase on increasing the surfactant concentration. A lamellar phase is observed at higher surfactant concentrations. X-ray diffraction studies on these systems reveal a diffused peak at small angles in addition to the set of peaks which arises due to the lamellar periodicity. Since the ionic conductivity measurements do not show a discontinuity across the nematic to lamellar transition, it was proposed that the lamellar phase was made up of disk-like micelles arranged in layers [9]. However the scattering from such an array of disk-like micelles separated by a continuous medium cannot be distinguished from the scattering from water filled pores in a continuous bilayer. Further experimental studies were carried out on these systems using small angle neutron scattering techniques as well as water diffusion experiments on oriented bilayers [10]. They showed that the bilayers consist of pores filled with water. The pores heal on adding $CsCl_2$ or on increasing the surfactant concentration, to form a lamellar phase without defects.

Such curvature defects are also found in mixed-surfactant systems [11]. Neutron scattering studies on SDS-alcohol-water system find that the number of defects per unit area increases as the SDS/alcohol ratio increases. However the pores disappear gradually when the water content is decreased. . Similar defects occur in mixtures of dimyristoylphosphatidyl choline (DMPC) with a shorter chain lipid dihexanoylphosphatidyl choline (DHPC) [12]. These mixtures form disk-like aggregates called bicelles at low surfactant concentrations. Small angle neutron scattering studies show that at higher temperatures, they form a lamellar phase consisting of bilayers with pores. These pores are expected to arise when DHPC phase separates to the edges of the bilayer or to the rim of the pores.

There have also been some theoretical studies on curvature defects in bilayers, which predict a transformation from stripes to random lines to pores on increasing the surfactant concentration [13]. The stripe phase consists of slits in the plane of the bilayer, parallel to each other. The random lines are obtained as the slits meet leading to random cuts in the plane of the bilayer. The pores form as the slits within each bilayer close upon themselves. The origin of these defects may be qualitatively understood as follows. Each defect or pore is made of a semitoroidal rim or edge. If the amphiphile locally prefers a curved surface as compared to a flat region, the overall free energy of the system can be lowered by the creation of these edges or pores in the bilayer. The surfactants that would have occupied the pores can be accommodated in two ways: i) by decreasing the area per surfactant molecule in the bilayer; this leads to a stretching of the tails of the amphiphiles and hence to an increase in the thickness of the bilayers, ii) by creating more bilayers; this however decreases the interlamellar separation. Thus creation of pores decreases the packing entropy. If the surfactants are charged, as in the CsPFO-water system, the electrostatic repulsion between the edges in adjacent bilayers also cost energy, as the surfactant concentration increases. Hence at lower water content, when the interlamellar interactions become significant, the pores disappear. The increase in the density of defects, as the SDS/alcohol ratio increases indicate that SDS prefers curved regions locally. This may also lead to a phase separation of the SDS and alcohol molecules with further loss of entropy.

2.5 Discussion

The isotropic phase at $\alpha \sim 0.25$ consists of worm-like micelles. This is indicated by the high viscosity as well as by the flow birefringence observed on shearing these samples. The growth of these long flexible micelles is the consequence of the decrease in the spontaneous curvature of the CTAB cylinders in the presence of SHN. CTAB forms a hexagonal phase over a wide range of surfactant concentration. Therefore, the observation of a hexagonal phase at low SHN concentrations ($\alpha \sim 0.25$) is not surprising. However at very low water

content a crystalline phase is obtained at 30^oC, since the Kraft temperature of CTAB increases with surfactant concentration [14]. The rectangular phase at 50^oC obtained at $\phi_s \sim 0.7$, is usually observed in surfactant systems in between the hexagonal and lamellar phases as the water content is lowered. This is formed by long aggregates with an almost elliptical cross-section, known as ribbons. These ribbons are arranged on a 2D rectangular lattice. At higher surfactant concentrations the ribbons merge to form bilayers, thus leading to a lamellar structure.

The isotropic phase at $\alpha \sim 0.43$ could be made up of long rod-like micelles, since the viscosity of these mixtures is found to be higher than that of the lamellar phase. The formation of an isotropic, viscoelastic gel on heating from the L_α phase at higher surfactant concentration, indicates that vesicular aggregates undergo a change in shape to form long flexible rod-like micelles that get entangled.

The observation of the lamellar phase at higher surfactant concentrations, is in confirmation with earlier studies on dilute mixtures of CTAB-SHN. However we find that the lamellar phase occurs earlier, that is, at a lower ϕ_s on increasing α. In the diffraction pattern of the oriented sample, the orientation of the diffused peak perpendicular to the lamellar peaks indicate that they arise from some structure in the plane of the bilayer. The diffused peaks observed here have been reported earlier in a few surfactant systems where they are believed to arise from pores in the plane of the bilayer, as discussed in section 2.4. Hence we surmise that in the CTAB-SHN system also curvature defects are present in the plane of the bilayer. Since no x-ray diffraction studies have been carried out till now, this is the first report of these defects in the present system. The isotropic solution at $\alpha \sim 0.67$ is most probably made up of vesicles since the viscosity of the solution is found to be low.

The lamellar phase exists over a wide range of surfactant concentration at $\alpha \sim 0.67$, indicating the existence of long range repulsion between the bilayers which allows them to swell.

One possible origin of such a repulsion is electrostatic interaction between the charged bilayers. The interaction energy per unit area between two planar surfaces of charge density σ, separated by a distance z is given by [15]

$V_{el}(z) = \frac{2\sigma^2\lambda_D}{\epsilon\epsilon_o}e^{-z/\lambda_D}$

where σ is the surface charge density, λ_D the Debye length, ϵ and ϵ_o, the dielectric constant of the medium and the dilelectric permittivity of free space respectively. If χ is the ionic strength of the solution, then $\lambda_D = [\frac{\epsilon\epsilon_o k_B T}{4\pi\chi e^2}]^{\frac{1}{2}}$. k_B is the Boltzmann constant and T the temperature.

In the lamellar phase of CTAB-SHN-water system, due to the release of the Br^- and Na^+ counter ions into the solution, the effective salt concentration is high and the Debye length is < 1 nm. On the other hand, the thickness of the water layer separating the bilayers is > 2 nm. Therefore, electrostatic repulsion between adjacent bilayers in the lamellar phase can be expected to be negligible and cannot account for the observed swelling behaviour.

The other possible origin of the interbilayer repulsion is the steric interaction between the bilayers due to thermal undulations of the bilayers [16]. The steric interaction energy per unit area between two bilayers separated by a distance z is

$V_u(z) = 3\,\pi^2\,(k_BT)^2/128\kappa\,z^2$

where κ is the rigidity modulus of the bilayer, k_B the Boltzmann constant and T the temperature. This repulsive interaction can be increased either by increasing the temperature or by increasing the flexibility of the bilayers. The addition of alcohol is known to lower the bending rigidity of bilayers by an order of magnitude [17]. This in turn is found to increase the bilayer separation by two orders of magnitude. Since the electrostatic interactions can be ruled out in the CTAB-SHN-water system, we surmise that a steric repulsion, stabilizes the lamellar phase over a large range of surfactant concentration. It would indicate that the CTAB-SHN bilayers are highly flexible, but we have not measured κ independently.

The absence of any shift in the peak positions in the diffraction pattern on increasing the temperature indicates that the separation between the bilayers as well as the separation between the defects in the plane of the bilayer do not change up to 60^o C. This leads us to conclude that the defect density does not alter with temperature. No clear picture exists at present regarding the structure of these defects. Since the defects are not oriented in the plane of the bilayer, it is difficult to extract any information regarding the form factor of these defects from the x-ray diffraction data. Hence it is not known whether these defects are pores or long slits in the plane of the bilayer. The size distribution of the defects, that is whether the pores or slits are polydisperse or monodisperse is also not known. But the presence of the ribbon phase at higher surfactant concentration indicates that these are most probably slits.

The appearance of multilamellar vesicles at low surfactant concentration in equimolar mixtures has not been understood at present. Also, the interlamellar separation increases as the surfactant concentration increases. Since one molecule of NaBr is released for every CTAB and SHN that associate to form a complex, the increase in surfactant concentration leads to the increase in the salt concentration in the surfactant solution. Swelling of the bilayers on increasing surfactant concentration is possibly due to the presence of salt. More work has to be done to understand this behaviour.

The formation of a centered rectangular structure in between the two lamellar phases is unusual. As far as we know, the CTAB-SHN-water system is the first to show such a behaviour. Normally the centered rectangular phase (R) appears in between the hexagonal and lamellar phases, similar to the behaviour observed in our system at $\alpha = 0.25$ described above. A 2D centered rectangular lattice can result if trans-bilayer correlations arise between the defects. 3D lattices of such defects have been observed in some lipid-polypeptide systems [18]. If the defects formed a centred rectangular structure, one of the lattice parameters would correspond to twice the lamellar periodicity. If we consider the lattice parameters of our system in the centred rectangular phase, say at α =0.67, $\phi_s = 0.55$, the lattice parameters

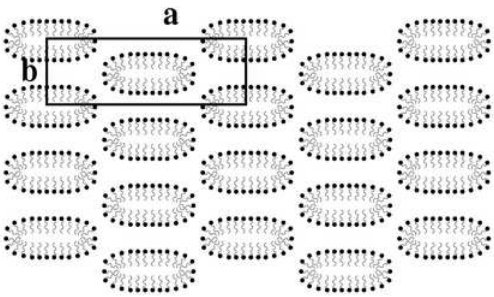

Figure 2.15: Schematic of the structure of the centred rectangular phase of CTAB-SHN-water system consisting of ribbon-like micelles arranged on a 2D rectangular lattice.

are found to be 14.04 nm and 5.84 nm. The periodicity of the lamellar phase at α=0.67, ϕ_s = 0.525 is 5.49 nm. Thus twice the lamellar periodicity of the lamellar phase close to the $L_\alpha^D \rightarrow$ R transition is not comparable to the lattice parameters observed in the centred rectangular structure. Moreover, in such a structure, the strongest reflection in the x-ray diffraction data would be from the (2 0) planes, which corresponds to the scattering from the bilayers and not from the (1 1) planes as observed here. Hence we can rule out a lattice arising from the 2D ordering of defects. This indicates that the centred rectangular structure seen here most probably consists of ribbon-like aggregates arranged on a 2D centred rectangular lattice (fig 2.15). Such structures have been seen before in some surfactant systems in between the hexagonal and lamellar phases [7].

The decrease in the separation between defects in the plane of the bilayer on increasing the SHN concentration indicates an increase in defect density. The fact that we find the centred rectangular phase at a lower surfactant concentration on increasing SHN concentration may be related to this. An increase in the defect density above a critical value, may lead to the formation of ribbon-like aggregates that form a 2D lattice. Further theoretical work is needed to understand this behaviour.

The absence of a diffuse peak in the lamellar phase at high surfactant concentrations

(L_α), indicates that the defects are absent in the plane of the bilayer. The transformation from a lamellar phase with defects (L_α^D) to one without defects (L_α) at high temperatures (fig 2.9,2.10,2.13) is similar to the behaviour seen in some surfactant systems, discussed in section 2.4. However the appearance of a centred rectangular phase (R) in between the two lamellar phases at lower temperatures cannot be understood in the framework of present theories.

2.6 Conclusions

Partial phase diagram of the tertiary system CTAB-SHN-water has been constructed. In addition, temperature-composition phase diagrams of the system at a few values of [SHN]/[CTAB] have also been determined. We find that the phase behaviour of this system is rather rich consisting of hexagonal, lamellar, oblique and centred rectangular structures. The $L_\alpha^D \rightarrow$L$_\alpha$ transformation that we observe here at high temperatures has been seen earlier in some surfactant systems. However the $L_\alpha^D \rightarrow$ R $\rightarrow L_\alpha$ transition at lower temperatures has not been reported in any other surfactant system.

Bibliography

[1] B. K. Mishra, S. D. Samant, P. Pradhan, S. B. Mishra, and C. Manohar, Langmuir **9**, 894 (1993).

[2] M. E. Cates and S. J. Candau, J. Phys. Condensed Matter **2**, 6869 (1990).

[3] R. A. Salkar, P. A. Hassan, S. D. Samant, B. S. Valaulikar, V. V. Kumar, F. Kern, S. J. Candau, and C.Manohar, Chem. Commun. **10**, 1223 (1996).

[4] E. Mendes, J. Narayanan, R. Oda, F. Kern, S. J. Candau, and C. Manohar, J. Phys. Chem. B **101**, 2256 (1997).

[5] K. Horbaschek, H. Hoffmann, and C. Thunig, J. Colloid Interface Sci. **206**, 439 (1998).

[6] C. A. Baker, D. Saul, G. J. T. Tiddy, B. A. Wheeler, E. Willis, J. Chem. Soc., Faraday Trans. **70**, 154 (1974).

[7] Y. Hendrikx and J. Charvolin, J. de Physique **42**, 1427 (1981).

[8] M. S. Leaver and M. C. Holmes, J. Phys. II France **3**, 105 (1993).

[9] M. C. Holmes, D. J. Reynolds, and N. Boden, J. Phys. Chem. **91**, 5257 (1987).

[10] M. C. Holmes, P. Sotta, Y. Hendrikx, and B. Deloche, J. Phys. II France **3**, 1735 (1993).

[11] Y. Hendrikx, J. Charvolin, P. Kekicheff, and M. Roth, Liq Cryst. **2**, 677 (1987).

[12] M. Nieh, C. J. Glinka, S. Kroeger, R. S. Prosser, and J. Katsaras, Langmuir **17**, 2629 (2001).

[13] C. K. Bagdassarian, D. Roux, A. Benshaul, and W. M. Gelbart, J. Chem. Phys. **94**, 3030 (1991).

[14] X. Auvray, C. Petipas, R. Anthore, I. Ricco, and A. Lattes, J. Phys. Chem. **93**, 7458 (1989).

[15] J. N. Israelachvili, *Intermolecular and Surface Forces*, 2nd edition, Academic Press, London (1991).

[16] W. Helfrich, Z. Naturforsch **33a**, 305 (1978).

[17] C. R. Safinya, E. B. Sirota, D. Roux, G. S. Smith, Phys. Rev. Lett. **62**, 1134 (1989).

[18] L. Yang, T. M. Weiss, R. I. Lehrer, and H. W. Huang, Biophys. J. **79**, 2002 (2000).